Study of Polyethylene Photodegradation in Formulations with a System of Interacting Photostabilizers and Antioxidants

M. L. BERLANGA-DUARTE, J. L. ANGULO-SÁNCHEZ,* and M. C. GONZÁLEZ-CANTÚ

Centro de Investigación en Química Aplicada (CIQA), Blvd. Enrique Reyna 140, Saltillo, Coahuila, México 25100

SYNOPSIS

The accelerated UV photodegradation process of low-density polyethylene films, formulated with two photostabilizers and two antioxidants, was studied to evaluate the effect of different combinations of UV stabilizers and antioxidants on the overall photodegradation process. An experimental design, consisting of 33 formulations with different additive ratios and a blank, was used to evaluate the performance of the four mixed additives. From each formulation, 200 micron-thick films were produced by the extrusion-blowing process. Samples from these films were submitted to accelerated UV aging, and the polymer degradation was measured by carbonyl group evolution, molecular weight distribution changes, and maximum elongation loss. The effect of the additive combination on the different degradation reactions is discussed qualitatively by using "relative variables" and a triangular diagram. © 1996 John Wiley & Sons, Inc.

INTRODUCTION

Polymer photodegradation is an intensive field of study, but most of the published articles dealt with only one type of measurement (chemical or mechanical) to evaluate the degradation and mainly with one type of stabilizer (photostabilizer or antioxidant); only a few articles studied the degradation by several methods or use combinations of one antioxidant and one photostabilizer. From the latter type of studies, the synergistic and antagonistic behavior of some additives[1,2] were determined; good examples of synergistic interactions are those observed in the case of hindered amine light stabilizers (HALS)[3] with UV absorber benzophenones[4] and those between hindered phenols and phosphites. On the other hand, antagonism was observed[5] when HALS are mixed with sulfur-containing compounds in polypropylene. Apparently, there are no reports analyzing the influence of the presence of more than two additives, although reports on the behavior of commercial films formulated with several (not specified) additives have been published. It is worth noting at this point that, actually, it is impossible to predict which systems will present synergism or antagonism; hence, to develop interacting systems, work has been focused on the use of compounds with chemical structures similar to those in which these types of behavior were observed.

On the practical side of photostabilization, long-lasting films of low-density polyethylene (LDPE) for outdoor purposes (mainly agriculture) were obtained by the combination of different additives, antioxidants, and UV stabilizers, but although the photodegradation process in polyethylene is, perhaps, the most studied, we were not able to find reports on the effect of the combination of several stabilizers on the degradation routes.

This work reports on the analysis of the combined action of four additives, with reported synergistic interaction by pairs (between two antioxidants and between two UV stabilizers), on the accelerated UV degradation process of LDPE films. The degradation process is evaluated by measuring the changes in chemical structure (carbonyl evolution, chain scission, and recombination) as well as mechanical characteristics (tensile properties) loss. For this purpose, a series of 33 formulations with different additive ratios and concentrations were designed, using a faced-centered-composite

---

* To whom correspondence should be addressed.

Table I Reported Protection Mode (11–14) for the Additives Used in This Study

Additive Type	Chemical Family	Action Mode
Antioxidant (primary)	Hindered phenol	Free-radical scavenger
Antioxidant (secondary)	Phosphite	Hydroperoxide deactivator
Photostabilizer	Hydroxybenzophenone	UV absorber
Photostabilizer	Hindered amine	Free-radicals scavenger and hydroperoxide deactivator

experiment design, based on the reports of other authors[6-8]; a LDPE film without additives, but processed under the same conditions as the formulated samples, was used as a blank. Finally, a commercial film was included for comparison purposes. The chemical change was determined by FTIR and size-exclusion chromatography (SEC), while the elongation-at-break (E_B) reduction was determined by stress–strain measurements. A qualitative discussion on the possible degradation reactions modified by the combined action of the four additives is presented.

EXPERIMENTAL

Polymer

Mexican commercial LDPE synthesized by Petroleos Mexicanos (PEMEX), code LDPE PX 22004X, was used as received. The measured physical characteristics are melt flow index 0.56 g/10 min (ASTM D-1238 [Ref. 9], 90°C temperature, and 2060 g load), density of 0.92 g/cm³ by the gradient column method ASTM 1505,[10] and molecular weight averages of M_n = 44,000 and M_w = 272,000 ± 5%, determined by size-exclusion chromatography (SEC).

Additives

Commercial antioxidants: Hindered phenol (MW = 1178) and phosphite (MW = 646.9) were purchased from CIBA-GEIGY and used as received. A

polymeric hindered amine (MW = 2285) from CIBA-GEIGY and hydroxybenzophenone (MW = 326.21) from Cyanamid were used as ultraviolet stabilizers. The principal action mode of these additives in the degradation process[11-14] is noted in Table I.

Commercial Polyethylene Film

A Spanish commercial film (Alcudia CP 117) designed for agriculture applications (greenhouse covering) was used as a reference (sample CT).

Sample Design

A faced-centered-composite design with four variables (one per additive) was used. A total of 33 formulations and a blank were defined for the evaluation of the performance formulation; details on the structure of the model will be given elsewhere. All formulations had the four additives in different ratios and total concentration, and four of them were used as replications to evaluate the reproducibility of the experiment. Three concentration levels for the additives were used in the experiment design (Table II). The individual additive concentrations for each formulation are presented in Table III.

Films and Samples Preparation

Additive incorporation into the polymer was carried out in an internal mixer (Brabender PL 2000), with

Table II Additives Concentration Range Used in the Formulations

Additive	Concentration (phr)		
	Minimum	Medium	Maximum
Hindered phenol	0.05	0.075	0.1
Phosphite	0.05	0.225	0.4
Hydroxybenzophenone	0.05	0.275	0.5
Hindered amine	0.1	0.3	0.5

Table III   Additive Concentration by Formulation

Formulation No.	Additives Concentration (phr)			
	Hindered Phenol	Phosphite	Hydroxybenzophenone	Hindered Amine
1	0.00	0.00	0.00	0.00
2	0.05	0.40	0.05	0.50
2a	0.05	0.40	0.05	0.50
2b	0.05	0.40	0.05	0.50
3	0.05	0.40	0.05	0.10
4	0.05	0.40	0.50	0.10
5	0.05	0.40	0.50	0.50
6	0.05	0.225	0.05	0.10
7	0.05	0.05	0.05	0.10
8	0.05	0.05	0.50	0.10
9	0.05	0.05	0.05	0.30
10	0.05	0.05	0.05	0.50
11	0.05	0.05	0.50	0.50
12	0.05	0.225	0.275	0.10
13	0.075	0.40	0.275	0.30
14	0.075	0.225	0.275	0.10
15	0.075	0.225	0.305	0.30
16	0.075	0.225	0.275	0.30
16a	0.075	0.225	0.275	0.30
16b	0.075	0.225	0.275	0.30
17	0.075	0.225	0.50	0.30
18	0.075	0.225	0.275	0.50
19	0.075	0.05	0.05	0.10
20	0.075	0.05	0.275	0.30
21	0.10	0.40	0.05	0.10
22	0.10	0.40	0.50	0.10
23	0.10	0.40	0.05	0.50
24	0.10	0.40	0.50	0.50
25	0.10	0.225	0.275	0.30
26	0.10	0.05	0.05	0.10
27	0.10	0.05	0.50	0.10
28	0.10	0.05	0.05	0.50
29	0.10	0.05	0.50	0.50
30	0.50	0.225	0.275	0.30

Cam rotors, 60 rpm angular velocity, $170 \pm 2°C$ temperature, and 12 min total mixing time. The irregular-shaped pieces recovered from the mixer were cut and reprocessed in an extruder (Killion, with a 2.54 cm diameter screw, L/D 3 : 1; circular die; and an adequate temperature profile for processing polyethylene) to obtain approximately cylindrical pellets 2 mm diameter $\times$ 5 mm length. These pellets were used to produce film by feeding them to a Betol extrusion-blow equipment Model 32/25 having an L/D = 25 : 1 screw and annular die of 2.54 cm diameter. The temperature profile was 140, 170, 190, and 220°C at the four-barrel zones and 220 and 215°C at the two die zones. The extrusion-blow parameters were adjusted to produce films with a blow ratio of 2.0 and 200 microns thickness. From these films, samples 12 $\times$ 6 cm were cut and submitted to accelerated UV aging.

Accelerated UV Aging

The film samples for UV aging were placed in the irradiation chamber of an accelerated UV instrument, (Q-Panel, Model QUV) having eight fluorescent lamps with maximum emission at 280–315 nm. The chamber was operated according to the ASTM D-4329-84 method,[15] selecting 4 h condensation/UV-irradiation cycles, at 40/60°C temperature, respectively. From the chamber, samples for analysis were extracted at different times depending on the formulation. Table IV shows the days of exposure and time code for each formulation.

Table IV Sampling Days for the Accelerated UV Aging of the Formulation

Formulation No.	T0	T1	T2	T3	T4	T5	T6	T7	T8
1	0	7	10	14	—	—	—	—	—
2	0	7	14	35	42	56	79	83	—
2a	0	14	28	42	56	70	83	98	112
2b	0	14	28	42	56	70	83	105	112
3	0	17	31	45	55	73	—	—	—
4	0	14	28	42	56	70	99	119	133
5	0	14	35	56	77	91	112	133	154
6	0	14	35	56	77	91	—	—	—
7	0	16	30	44	56	—	—	—	—
8	0	7	14	21	35	49	56	77	84
9	0	14	35	54	—	—	—	—	—
10	0	14	32	46	53	67	85	99	112
11	0	14	35	56	77	98	119	154	161
12	0	14	35	56	77	91	119	140	—
13	0	14	35	49	63	77	98	126	161
14	0	14	28	49	70	84	98	112	133
15	0	14	28	49	63	77	98	119	133
16	0	14	28	49	70	84	91	105	119
16a	0	14	28	49	70	84	98	—	—
16b	0	14	28	49	84	98	112	126	—
17	0	14	28	49	70	105	119	140	168
18	0	14	28	49	63	83	98	—	—
19	0	14	35	56	70	84	98	112	—
20	0	14	28	49	77	84	98	112	133
21	0	14	21	35	63	84	—	—	—
22	0	14	28	42	63	84	98	112	133
23	0	14	28	42	59	—	—	—	—
24	0	7	14	21	35	42	59	77	—
25	0	14	28	49	77	84	98	112	133
26	0	14	28	42	56	—	—	—	—
27	0	14	28	42	56	70	84	—	—
28	0	7	14	21	35	42	56	79	83
29	0	14	28	42	56	79	83	98	112
30	0	14	28	49	77	84	98	112	140
CT	0	19	33	55	75	98	—	—	—

Degradation Measurements

Polymer degradation was measured as a function of irradiation time by (1) chemical changes (carbonyl group evolution and molecular weight change) and (2) mechanical testing (maximum elongation loss).

Chemical Changes

The carbonyl group formation and the molecular weight decrease were measured by FTIR and SEC, respectively. The infrared measurements were carried out in an FTIR instrument, (Nicolet 710) and a carbonyl index (CI) was calculated according to the following equation[16]:

$$CI = (A/e \times EC) \times 100 \qquad (1)$$

where A is the absorbance of the signal at 740 cm^{-1}; EC, the extinction coefficient; and e, the film thickness.

The molecular weight distributions (MWD) of 16 selected formulations were measured by SEC in a Waters 150C chromatograph equipped with refractive index detector and a set of three Ultrastyragel columns with nominal porosity 10^6 and 10^4 Å and a linear mixture; the carrier solvent was 1,2,4-trichlorobenzene at 140°C temperature and 1 mL/min flow rate. Molecular weight averages were calculated using a universal calibration curve constructed with narrow MWD polystyrene standards and the reported[17] Mark–Houwink constants (K = 5.17 $\times$ 10^{-4} dL/g, a = 0.706) for polyethylene. The changes in molecular weight averages are related to

the ratio between the fraction of main chain scissions (po), and fraction of crosslinked chains (qo), in such a way[18] that if $po/qo > \frac{1}{2}$, M_n decreases, and if $po/qo < \frac{1}{2}$, M_n increases; on the other hand, if $po/qo > 2$, M_w decreases, and if $po/qo < 2$, M_w increases. The average number of scissions per polymer chain (n) is defined[18] by the following equation:

$$n = (M_{n_0}/M_{n_t}) - 1 \qquad (2)$$

where M_{n_0} = initial number-average molecular weight and M_{n_t} = number-average molecular weight after exposure time t.

Mechanical Testing

Tensile tests were carried out using a universal testing machine (Instron 1122, according to ASTM D-882)[19] on 1×10 cm specimens at $23 \pm 2°C$ and 200 mm/min crosshead speed. Plots of the retention percent on elongation at break E'_B against irradiation time were used to compare the different formulations' performance, E'_B being defined as

$$E'_B = (E_{B0}/E_{Bt}) \times 100 \qquad (3)$$

where E_{B0} and E_{Bt} are the initial elongation at break and after an irradiation time t for a given sample.

RESULTS AND DISCUSSION

The results for the carbonyl index (CI), molecular weight (M_w, M_n), polydispersity (M_w/M_n), and elongation at break (E_B) are presented in Tables V–VII and will be discussed separately.

Changes in Carbonyl Index with Irradiation Time

The CI was plotted against the squared irradiation time (t^2); in Figure 1, only three curves are shown (representative of the three different behaviors exhibited by all the samples) to avoid an excessive number of lines in the graph. The main features in this figure are as follows:

Case a: Practically no changes in CI on increasing irradiation time, shown by formulations 2, 2a, 2b, 4, 5, 8–12, 17, 20, 22, 23, and 26–29.

Case b: Induction time with no initial change in CI followed by a steep increase. This feature observed in formulations 1, 3, 6, 7, 13, 14, 16, 16a, 16b, 18, 21, and 24. The induction time for the blank (pure polymer) is very short, but

the curve is parallel to curve b; hence, it was included in this case.

Case c: No change in CI for a long time period after which there is a small increase that is rapidly reduced to form a small "hill" with a maximum; this behavior was exhibited by formulations 15, 19, 25, and 30. The maximum position depends on the formulation, being around 49, 70, 84, and 98 days for samples 15, 19, 25, and 30, respectively. The commercial film shows an increment on CI, but not as evident as with the samples in case b.

It is important to note that in all three cases, and despite the lack of carbonyl groups in case a, the polymer underwent degradation (as indicated by the loss of mechanical properties), this process being discussed later. The general behavior observed here shows that, in some cases, the use of the CI as the only parameter to evaluate the polymer degradation is not adequate.

Considering the 15 reactions (Fig. 2) reported to take place during the polyethylene photodegradation process,[18] it is possible to say that in case a the degradation must proceed by reactions leading to chain scissions (reactions IV, X, XI, and XII in Fig. 2). There are two options that would favor these reactions:

1. Blockage of the routes that generate carbonyl groups (reactions I, II, and III, in Fig. 2).
2. Acceleration of the chain scission reactions.

Considering the additive character in Table I (hydroperoxide decomposers and free-radical scavengers), the first proposition is more probable. The behavior does not depend on the total additive concentration, but most likely on additive combination, because the formulations showing this behavior include both low and high total concentrations containing the four additives, although in different ratios.

In case b, initially, the process may be similar to case a, but, later, the carbonyl-producing reactions (VI, VIII, and IX in Fig. 2) should dominate the process, leading to high CI values. Chain scissions can take place through Norrish I and Norrish II reactions, X and XI, in Figure 2. This suggests an antioxidant depletion in the formulation when carbonyl groups are generated, but the formulations showing this behavior had high antioxidant initial concentration and films formulated with lower antioxidant concentration did not behave the same.

Finally, in case c, the initial performance of the additive combination should be similar to case b, but the presence of a maximum suggests that there are not enough POOH or oxygen in the medium to

Table V Carbonyl Index (CI) Calculated with Eq. (1), at Different Exposure Times[a] and Half-life Time ($t_{1/2}$)

Formulation No.	T0	T1	T2	T3	T4	T5	T6	T7	T8	$t_{1/2}$
1	0.95	1.73	2.08	5.36	—	—	—	—	—	7
2	0.88	0.96	0.82	0.85	0.81	0.86	1.00	1.23	1.19	71
2a	0.86	0.91	0.83	1.25	0.96	1.05	1.22	1.25	1.47	84
2b	0.92	0.99	1.03	0.99	0.94	0.99	1.15	1.15	1.26	89
3	0.87	0.98	1.05	1.13	1.52	2.22	—	—	—	62
4	0.75	0.70	0.81	0.75	0.78	0.79	0.93	1.00	1.03	93
5	0.87	0.85	0.88	0.97	0.92	0.96	0.97	0.92	0.98	122
6	0.94	0.96	1.09	2.07	2.32	3.06	—	—	—	56
7	1.05	1.07	1.10	1.25	1.42	—	—	—	—	31
8	0.77	0.78	0.79	0.73	0.79	0.82	0.92	0.92	0.92	62
9	0.67	1.00	1.02	1.34	1.00	1.34	1.28	—	—	98
10	0.93	0.83	0.93	0.95	0.90	0.97	—	—	—	37
11	0.97	0.87	0.85	0.86	0.90	0.80	0.83	0.88	0.95	133
12	0.63	0.66	1.22	1.07	1.18	1.12	1.46	2.04	—	89
13	0.74	0.71	0.80	0.80	0.87	1.04	1.01	1.24	1.85	126
14	0.84	0.71	0.78	1.06	1.10	2.03	2.15	3.06	6.87	77
15	0.69	2.25	2.31	3.79	1.35	0.95	1.21	1.03	1.29	75
16	0.75	0.64	0.66	0.98	1.14	2.35	2.92	3.52	—	85
16a	0.80	0.69	0.72	1.04	1.23	5.01	3.14	—	—	66
16b	0.63	0.90	0.97	1.34	1.50	1.50	1.67	1.85	—	101
17	0.68	0.82	1.03	1.08	1.41	1.18	1.33	1.39	1.70	160
18	0.94	0.72	0.77	1.15	1.26	6.22	7.29	—	—	69
19	0.65	1.02	1.44	1.19	3.30	1.80	2.89	—	—	56
20	0.75	0.80	0.91	0.85	0.88	1.12	1.22	1.28	1.29	120
21	0.95	0.90	0.98	1.14	1.11	2.26	—	—	—	54
22	0.81	0.82	0.82	0.83	0.80	0.88	0.96	1.02	1.19	96
23	0.82	0.96	0.93	0.94	1.01	—	—	—	—	49
24	0.80	0.87	0.99	0.86	0.88	0.95	1.10	1.08	1.11	64
25	0.93	0.89	0.89	0.96	0.98	2.03	1.40	1.62	1.48	101
26	0.76	0.92	0.88	0.92	0.99	—	—	—	—	47
29	0.99	0.94	0.92	0.92	0.98	0.98	0.85	0.90	1.01	91
30	1.24	1.11	0.95	1.12	1.13	1.33	2.45	1.58	1.73	100
CT	0.72	0.89	0.97	1.19	1.53	5.81	—	—	—	66

[a] Time in days, presented in Table IV.

continue the carbonyl formation. This supports the discussion in case b about not being due to antioxidant depletion, and, possibly, the Norrish reactions dominate the final process, as suggested by the reduction in molecular weight and elongation.

Changes in Molecular Weight

Table VI shows the changes in molecular weight averages and polydispersity (M_w/M_n) of selected samples. There are three measurements, corresponding to the initial stage (where $t = 0$ and $E'_B = 100\%$) and to the points where the samples had lost 50 and 80% of its elongation at break (second and third values, respectively). These values are independent of the time required to achieve the spec-

ified degradation condition. The changes may be correlated with the scission/recombination process; if degradation is dominated by polymer chain scissions, the molecular weight will be lowered, while if recombination is the main process, an increment of molecular weight and microstructure changes (branching crosslinking and eventually gel formation) will take place.[20] The results of molecular weight change will be discussed later, when simultaneously considering the three variables.

Elongation-at-break (E_B) Loss

The E_B change as a function of irradiation time is very similar to that reported by other authors (see,

Table VI   Molecular Weight Averages (M_w and M_n) at Different Elongation Loss Percentages, Determined by SEC

Sample	$M_w \times 10^{-3}$			$M_n \times 10^{-3}$			Polydispersity		
	0%	50%	80%	0%	50%	80%	0%	50%	80%
1	272.0	255.2	79.3	93.8	40.8	3.4	6.2	6.2	11.7
2	301.9	238.0	236.0	39.1	55.9	55.0	7.7	4.2	4.3
2a	256.0	181.3	172.5	44.5	43.4	39.8	5.7	4.2	4.3
2b	272.4	129.4	121.9	48.2	46.3	32.7	5.6	2.7	5.7
3	243.5	127.4	126.0	45.2	28.4	34.6	5.3	4.4	3.6
4	227.6	237.4	106.1	44.4	50.4	39.6	5.1	4.7	2.8
5	243.3	150.0	93.7	43.6	49.8	16.8	5.5	3.0	5.5
7	277.2	177.6	10.1	42.4	7.1	5.1	6.4	24.0	19.6
8	228.0	204.0	188.0	48.1	44.0	51.6	4.7	4.7	3.6
10	244.0	124.0	139.1	43.6	44.6	34.6	5.5	2.7	4.1
11	224.5	118.3	97.1	43.7	33.0	17.3	5.1	3.5	5.5
21	318.7	107.6	57.9	47.2	5.3	3.6	6.6	20.0	15.3
22	217.4	210.9	84.9	42.4	54.8	20.3	5.1	3.8	4.6
23	218.7	121.6	2.5	40.6	3.1	0.5	5.3	38.0	18.3
24	205.6	177.6	164.0	43.0	41.2	42.8	4.7	4.3	3.8
26	274.7	102.4	65.3	43.5	5.1	3.7	5.3	19.0	17.5
27	279.8	152.0	148.0	45.6	35.1	30.9	6.1	4.3	4.7
28	210.0	217.0	266.4	42.3	69.3	46.0	4.9	3.3	6.1
29	220.9	153.1	141.6	37.7	95.7	32.7	5.8	4.0	4.3
CT[a]	159.4	135.2	157.7	7.0	32.1	36.0	23.0	4.2	4.3

0%, 50%, and 80% are percentage of elongation-at-break loss.
[a] CT = commercial film.

e.g., Refs. 21 and 22) and essentially shows that E'_B decreases in value on increasing irradiation time; the curve span and curve shape depend on the formulation. The E_B results for all the formulations were plotted against irradiation time and the time required to reduce E_B to half its initial value ($t_{1/2}$) determined from these graphs. The $t_{1/2}$ results are included in Table V.

Half-life Time ($t_{1/2}$) as a Function of Additive Combinations

The half-life time is plotted as function of total additive (antioxidants plus ultraviolet additives) concentration in Figure 3; total antioxidant concentration, in Figure 4; and total UV additives, in Figure 5. In Figure 3, the half-lifetime shows a tendency to increase on increasing the total additive concentration. However, different values were obtained for the same total additive concentration which is due to the different amount of antioxidants and UV additives. The dotted line corresponds to the $t_{1/2}$ of the commercial film (66 days). It can be seen that high $t_{1/2}$ values can be achieved using relative low additive concentration and some combinations do not protect the film properly even at very high con-

centration. The behavior in Figures 4 and 5, $t_{1/2}$ plotted against total (hindered phenol and phosphite) antioxidant and total UV photostabilizers concentration, respectively, is similar to that observed in Figure 3, although the point order is not the same in these figures. For example, in Figure 5, the formulations containing 1 phr of photostabilizers show times between 64 and 133 days, and there is an apparent negative effect of the antioxidant concentration (c_{ao}), as for $c_{ao} = 0.1$ phr, $t_{1/2} = 133$ days; for $c_{ao} = 0.15$ phr, $t_{1/2} = 91$ days; and for 0.5 phr, $t_{1/2} = 64$ days, but for 0.45 phr, $t_{1/2} = 122$. The high values were obtained using 0.05 phr of phosphite antioxidant and the low values using 0.1 phr. On the other hand, for the 0.15 phr photostabilizer, the highest $t_{1/2}$ is achieved using $c_{ao} = 0.45$ phr, and the lowest, using $c_{ao} = 0.1$ phr; however, no direct correlation was observed with these or other combinations. This behavior reflects the interaction among the additives, antioxidants, and photostabilizers, but the correlations are yet under study by mathematical means.

Correlation Between the Three Measured Variables, (E_B), CI, and n

To correlate the three variables CI, E_B, and n, we assumed a lineal dependence between them and de-

fined new "relative variable fractions" according to the equations

$$(E_B)_R = (wE_B)/((wE_B) + CI + n) \qquad (4)$$

$$(CI)_R = CI/((wE_B) + CI + n) \qquad (5)$$

$$(n)_R = n/((wE_B) + CI + n) \qquad (6)$$

satisfying the condition

$$(E_B)_R + (CI)_R + (n)_R = 1 \qquad (7)$$

Here, the R subindex stands for the relative variable and "$w = 0.01$" is a weight factor introduced to have similar magnitude quantities.

Table VII shows the values for the relative variables of the selected samples, for which molecular weight data were acquired. The n_R negative values are due to an increase in molecular weight with irradiation time possibly by chain recombination. A triangular diagram (ternary system) was used to plot the results (Fig. 6). In this diagram, each triangle apex represents 100% of the particular relative variable whose name is noted; the points in the area within the triangle are combinations of the three
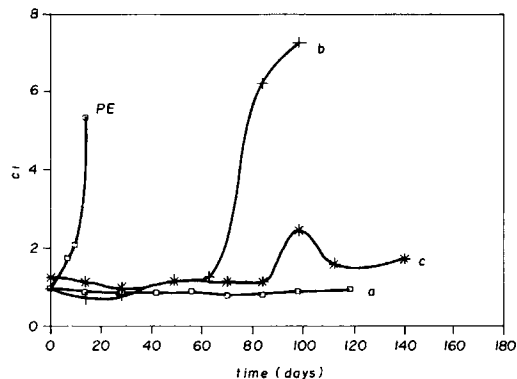

Figure 1 CI evolution as a function of UV irradiation time showing the three types of behavior exhibited by the formulations and pure polyethylene; see text.
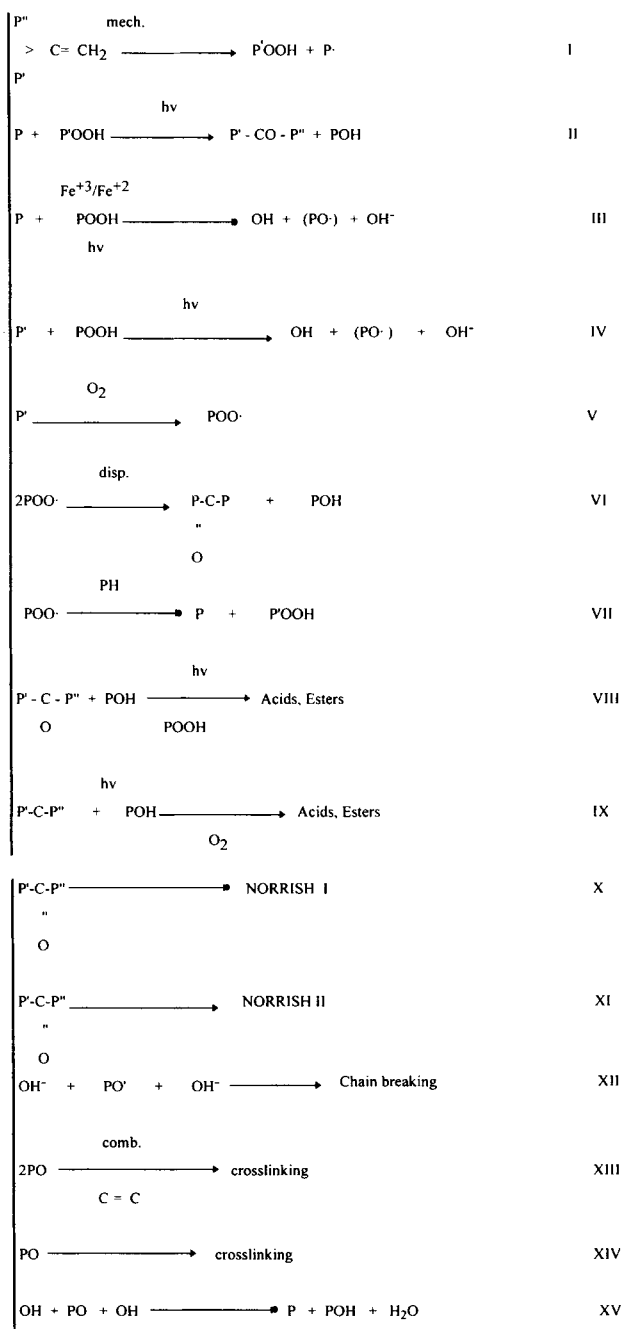
variables fulfilling the condition defined by eq. (7). Line d appears outside the triangle due to the negative n_R values. As an example, in Fig. 6, the relative values of the line c final point are marked as dotted lines, perpendicular to the side opposite to the apex with the variable name. In Figure 6, four lines (a–d) are shown, representing the behavior of all formulations. Two features are to be clarified in the figure: First,

Table VII Relative Variables [Calculated with Eqs. (4)–(7)] at Different Exposure Times, Determined at 0, 50, and 80% of Elongation Loss

Formulation No.	Carbonyl Index $(CI)_R$			Chain Scissions $(n)_R$			Elongation $(E_B')_R$		
	0%	50%	80%	0%	50%	80%	0%	50%	80%
1	2.22	9.45	21.85	0	0.28	44.22	97.7	90.2	33.9
2	1.91	4.45	12.02	0	−1.29	−2.93	98.0	96.8	90.9
2a	1.57	3.86	10.82	0	0.08	0.98	98.4	96.0	88.2
2b	1.82	4.44	10.75	0	1.81	4.10	98.1	93.7	85.1
3	1.96	6.38	19.78	0	2.48	2.72	98.0	91.1	77.4
4	1.48	3.93	10.51	0	−0.46	1.06	98.5	96.5	88.4
5	1.73	4.02	12.08	0	−0.47	0.59	98.2	96.4	87.9
7	2.53	4.08	8.46	0	18.85	43.23	97.4	77.0	48.3
9	1.54	3.22	8.63	0	0.37	−0.66	98.4	96.4	92.0
11	1.87	3.67	8.79	0	−0.08	2.35	98.1	96.4	88.8
12	1.68	3.39	10.62	0	1.22	1.31	98.3	95.3	89.3
21	1.85	3.25	9.49	0	23.18	48.51	98.1	73.5	41.9
22	1.60	3.97	9.77	0	−0.90	8.94	98.4	96.9	81.2
23	1.75	2.60	1.18	0	33.83	88.01	98.2	63.5	10.8
24	1.70	3.94	10.50	0	0.18	0.04	93.3	95.9	89.4
26	1.56	2.84	4.65	0	23.21	50.21	98.4	73.9	45.1
27	1.81	3.65	9.03	0	1.19	4.31	98.1	95.1	86.6
28	1.77	3.83	9.31	0	−1.46	−0.70	98.2	97.6	91.3
29	2.10	4.08	9.13	0	0.44	1.51	97.8	95.9	89.3
CT[a]	1.17	4.01	34.89	0	−2.58	−4.67	98.8	98.5	69.7

0%, 50% and 80% are percentage of elongation-at-break loss.
[a] CT commercial film.

P"   mech.
> C= CH$_2$ ─────────→ P'OOH + P·   I
P'

         hv
P + P'OOH ─────────→ P' - CO - P" + POH   II

     Fe^{+3}/Fe^{+2}
P + POOH ─────────→ OH + (PO·) + OH$^-$ III
         hv

              hv
P' + POOH ─────────────→ OH + (PO·) + OH$^-$ IV

      O$_2$
P' ─────────────→ POO·   V

      disp.
2POO· ─────────→ P-C-P + POH   VI
                      "
                      O
      PH
POO· ─────────→ P + P'OOH   VII

              hv
P' - C - P" + POH ─────────→ Acids, Esters   VIII
    O   POOH

         hv
P'-C-P" + POH ─────────→ Acids, Esters   IX
         O$_2$

P'-C-P" ─────────────→ NORRISH I   X
    "
    O

P'-C-P" ─────────────→ NORRISH II   XI
    "
    O
OH$^-$ + PO· + OH$^-$ ─────────→ Chain breaking   XII

         comb.
2PO ─────────────→ crosslinking   XIII
      C = C

PO ─────────────→ crosslinking   XIV

OH + PO + OH ─────────────→ P + POH + H$_2$O   XV

P, P' and P" represent different polymeric chains
P polymeric free radical.

Figure 2   Reactions occurring during the photodegradation of polyethylene.[18]

the final points for each line correspond to a loss in E_B of 80%, and, second, the lines do not pass through the "$E_B = 1$" apex, due to an initial value of the CI different from zero. In Figure 6, it is possible to see that any change in CI or n leads to a reduction of the elongation. Note that the trends in the figure are not directly related to those in Figure 1 due to the molecular weight change.

The type a line (Fig. 6) reflects the behavior of formulations 7, 21, 23, and 26; Here, CI remains constant, but the chain scissions (n) increase sharply, and, hence, elongation is reduced. This suggests that there is not an important oxidation process and that the reduction in E_B is mainly a consequence of n. Chain breaking can take place via Norrish I and II (reactions X and XI, Fig. 2). In this process, CO is eliminated, consuming the possible carbonyl groups present and generating two, end-carbon, free radicals which can react with oxygen and promote more scissions.[23] Alternatively, chain scission without carbonyl group formation can take place (reactions IV and XII, Fig. 2); with the present information, it is not possible to say if only one or both alternatives are occurring. On the other hand, the ester and acid formation (reactions VIII and IX) require the presence of oxygen and ketonic groups; this may be absent considering that HALS and the phosphite are oxygen and hydroperoxide deactivators. Based on this information, it is possible to assume that the HALS and phosphite are controlling the behavior.

The type b line, defined by the formulations 3–5, 8, 10, 11, 24, and 29, show an E_B reduction on increasing CI, but only minor changes in n; this fact suggests that the mechanical properties' reduction, in this case, is due mainly to polymer oxidation. We believe this, apparently constant, value of molecular weight is the result of an equilibrium between the chain scission and recombination events rather than a non-chain-breaking degradation mechanism. Besides, recombination of the polymer chains would yield branched molecules with reduced mechanical properties.

The case for the type c line (observed in formulations 22, 27, and the blank) is apparently a combination of the two previous behaviors, where the type b process dominates at early times, while the type a process overcomes it later. It is important to note here that, although the degradation scheme of both samples seems to be the same, the time required to achieve 50% loss in E_B is very different: 7 days for the blank and 96 and 70 days for the formulated samples.

Finally, type d behavior was shown by formulations 2 and 28 and the commercial sample. They exhibited a high oxidation process (high CI) and negative values for n, the last indicating that the recombination reactions dominate at early times, although an equilibrium between scission and recombination is achieved later, as the n value remains almost constant. No further analysis was possible for the commercial sample as the additives used for the stabilization of this film were unknown.
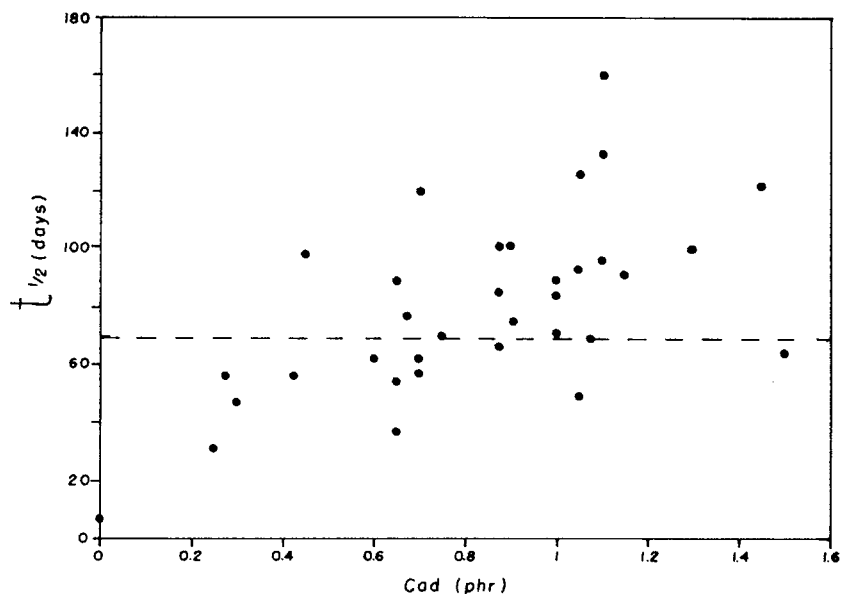
Figure 3 Different formulation-accelerated UV aging; half-life time as a function of total (antioxidants plus photostabilizers) concentration.

The results suggest that the reactions leading to the UV aging of the polymer may be retarded, but not totally eliminated. Aging characteristics are not a linear function of the additive type, ratio, or total concentration, because the half-life time cannot be obtained directly from them. Possibly, there are interactions, not defined, between all the additives that may explain this behavior, but further work is required to define them.

CONCLUSION

The results of UV-accelerated aging, measured as the elongation-at-break reduction in polyethylene films formulated with four additives (two synergistic pairs), are, in general, similar to those reported for the individual additives as far as the shape of the E_B vs. time curves is concerned.

The half-life times for the different formulations are a function principally of additive combinations rather than the total additive concentrations. This reflects the interaction between antioxidants and UV photostabilizers.

Despite the trend of the E_B vs. time plots and the fact that the same additives are present in all the formulations, the reaction pathways leading to polymer degradation are different, depending on the additive ratio and concentration. Analyzing the behavior of three relative variables, defined by eqs. (4)–(7) and plotted in Figure 6, four basic behaviors were identified:

1. The polymer degradation process apparently due to polymer chain scissions with only minor increase of CI, which suggests a retardation or blockage of the reactions leading to carbonyl formation (reactions V, VI, and IX, Fig. 2) or an acceleration of the chain scission reactions (IV, X, and XI, Fig. 2). Considering the additive action mode, the first option seems more appropriate.

2. Significant evolution of carbonyl groups, but few apparent chain scissions, indicating that the oxidation process is dominating the polymer degradation, i.e., there is a preference for reactions II, Va, Vb, VI, and VII in Figure 2. The apparent lack of scissions per polymer chain is most probably due to an equilibrium of the scission/recombination reactions rather than to a nonbreaking degradation mechanism. Independent of the apparent preservation of number-average molecular weight (M_n), the samples suffered a loss in elongation at break, indicating polymer degradation. This suggests that scission and recombination events are taking place and modify the polymer microstructure, in addition to oxidation, both being responsible for the mechanical properties loss.

3. Increase of the CI (maintaining a low number of chain scissions), followed by the CI leveling off, but increasing the number of chain scissions. We can considered this behavior as a combination of the previous two, one dominant
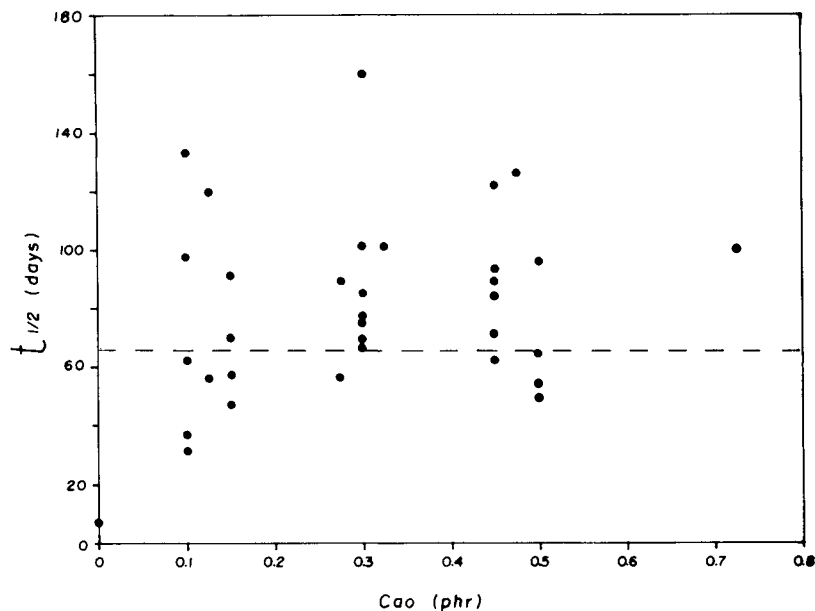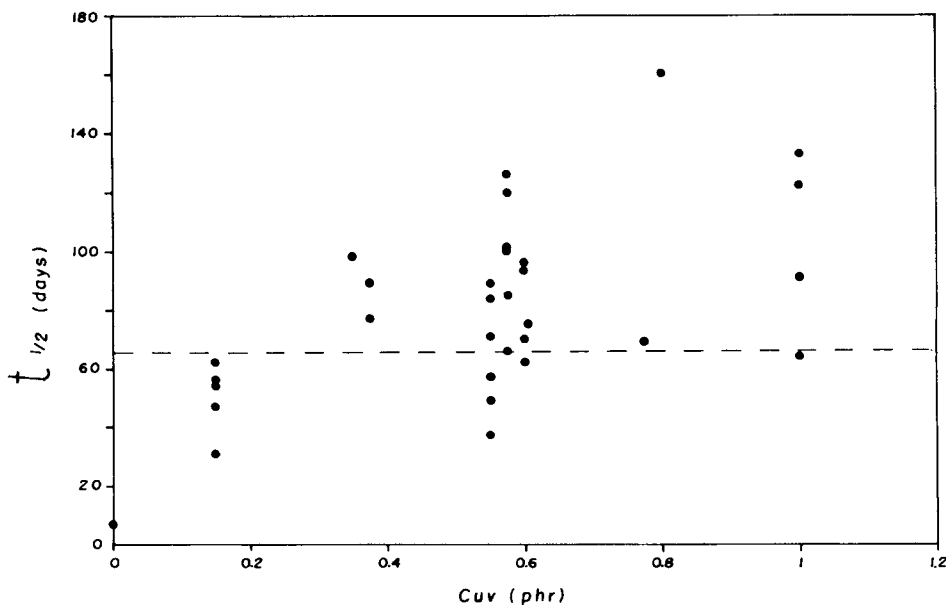
Figure 4   Different formulation-accelerated UV aging; half-life time as a function of total antioxidant concentration.

at early times of irradiation and the other later. The blank (pure polyethylene) and two formulations (with all four additives) exhibited this behavior; however, the time required to achieve 50% loss on maximum elongation (half-life-time) was over 10 times greater for the formulated sample.

4. CI increase, but negative values of chain scissions due to a molecular weight (M_n) increas-

ing. Here, the recombination reactions are the important event. Formulations 2 and 28 and the commercial film fit into this group.

The results indicate that the reactions occurring during UV irradiation and leading to polymer degradation are sensitive to the additive ratios as well as to the total concentration (C_T). In some cases, the influence of the additive ratio is stronger than

Figure 5   Different formulation-accelerated UV aging; half-life time as a function of total photostabilizer concentration.
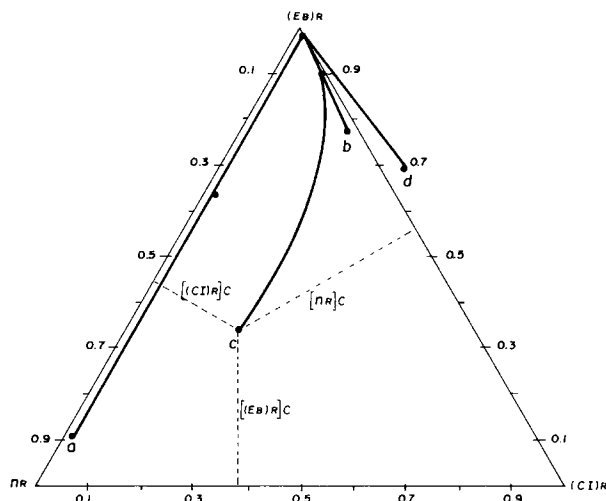
Figure 6   Triangular diagram plot of the relative variables defined by eqs. (4)–(7) showing that any changes in the number of chain scissions or carbonyl index promote the reduction of elongation at break.

is concentration; e.g., a longer lasting time (126 days) was found in formulation 13 than in formulations 4 and 23 whose half-life time were 93 and 49 days, respectively, both having the same total concentration of 1.05 phr.

The information collected up to the moment allowed us to identify formulations with better additive ratios, obtaining long-lasting films with a lower cost, based on the individual price of each additive. However, the optimal values (time/cost) cannot be obtained without the correlation between all the additives. The additive interaction degrees are under evaluation using mathematical methods.

REFERENCES

1. F. Catalina, N. S. Allen, and A. J. Chirinos Padron, *Rev. Plast. Mod.*, **416**, 197–203 (1991).
2. A. J. Chirinos Padron, *Rev. Macromol. Chem. Phys.*, **1**(30), 107–154 (1990).
3. T. Kurumada, H. Ohsawa, and T. Yamazaki, *Polym. Deg. Stab.*, **19**, 263–273 (1987).
4. A. J. Chirinos Padron, P. H. Hernandez, and N. S. Allen, *Polym. Deg. Stab.*, **19**, 177–189 (1987).
5. K. Kikkawa and Y. Nakahara, *Polym. Deg. Stab.*, **18**, 237–245 (1987).
6. T. D. Murphy, Jr., *Chem. Eng.*, **6**, 168–182 (1977).
7. J. W. Sell and S. Lepeniotis, *Adv. Polym. Tech.*, **11**(3), 193 (1992).
8. J. M. Minor, *Chem. Tech*, **Dec.**, 751 (1992).
9. ASTM D-1238, Flow Rates of Thermoplastics by Extrusion Plastometer, 1986.
10. ASTM D-1505, Density of Plastics by the Density Gradient Technique, 1985.
11. G. Scott, *Pure Appl. Chem.*, **52**, 365–387 (1980).
12. B. Khirud, K. B. Chakraborty, and G. Scott, *Eur. Polym. J.*, **13**, 1007–1013 (1977).
13. B. W. Evans and G. Scott, *Eur. Polym. J.*, **10**, 453–458 (1974).
14. F. Gugumus, *Plast. Univ.*, **4**, 220 (1985).
15. ASTM D-4329-84, Standard Practice for Operating Light- and Water-exposure Apparatus (Fluorescent UV-consideration Type) for Exposure of Plastics, 1984.
16. L. Martin-Vicente, S. Santolino-Martin, and G. Jorge-Tapia, *Rev. Plast. Mod.*, **292**, 465–472 (1980).
17. American Standards Corp. Catalog of Polymers Standards for Research and Development.
18. C. David, M. Trojan, A. Daro, and W. Demarteau, *Polym. Degrad. Stab.*, **37**, 233–245 (1992).
19. ASTM-D-882, Standard Tests Methods for Tensile Properties of Thin Plastic Sheets, 1983.
20. J. L. Angulo-Sanchez, H. Ortega-Ortiz, and S. Sanchez-Valdes, *J. Appl. Polym. Sci.*, **53**, 847–856 (1994).
21. S. Sanchez-Valdez and F. Orona, *Rev. Plast. Mod.*, **65**, 635–638 (1993).
22. S. Sanchez-Lopez, M. A. Uresti-Maldonado, and E. Ramirez-Vargas, *Rev. Plast. Mod.*, **41**, 363–368 (1991).
23. P. P. Klemchak, *Polym. Degrad. Stab.*, **27**, 183–202 (1990).